Computational Analysis of Experimental Results on Spatial Distributions of Fission Reaction Rates in the Annular Core of a Modular HTGR, Obtained at the ASTRA Critical Facility

V.F. Boyarinov[1], E.S. Glushkov[1], P.A. Fomichenko[1], G.V. Kompaniets[1], A.M. Krutov[1],
E.V. Marova[2], V.A. Nevinitsa[*1], D.N. Polyakov[1], O.N. Smirnov[1], Yu.P. Sukharev[2], A.A. Zimin[1]
[1] -Russian Research Center "Kurchatov Institute"
Institute of Nuclear Reactors, Moscow, Kurchatov sq.1
[2]- Experimental and Design Bureau of Machine Building,
Nizhny Novgorod, Burnakovsky proezd 15.

Abstract

The paper presents computational analysis of some experimental results on spatial distribution of ^{235}U fission reaction rates in a critical assembly with the annular core and different configurations of safety rods, placed into the inner reflector, made of graphite. Presented computational analysis of experimental data was performed with the set of codes used in HTGR design calculations.

KEYWORDS: HTGR with annular core, ASTRA critical facility, fission reaction rate.

1. Introduction

Nowadays the development of projects of High Temperature Gas Cooled Reactors (HTGRs) with gas turbines, such as GT-MHR with prismatic fuel assemblies (FA) in USA, Russia, France and Japan [1] or PBMR with spherical fuel elements in RSA [2], are widely carried out in the world. This type of reactor is expected to possess key advantages in safety because of the absence of core melting under the loss of coolant accident conditions.

A typical HTGR reactor with the annular core design has the following features which influence neutron physical characteristics:

1. Multilayer fuel coated particles placed in graphite matrix of fuel elements – this design causes so-called double heterogeneity of fuel arrangement in the core and thus requires validation of neutron-physical calculations with the use of results of integral experiments with fuel elements of similar type.
2. High value of "core height to core diameter" ratio (H/D=1.5…3), that causes high sensitivity of axial spatial power distribution to control rod axial positions and necessity of experimental study of the safety rods worth and their interference factor.
3. Annular core is characterized by high radial non-uniformity of power distribution with local power peaks at the boundaries of active core and side and inner graphite reflectors, etc.

---

[*] Corresponding author, Tel. +7 (495) 196-70-16, Fax. +7 (495) 196-70-16, E-mail: neva@dhtp.kiae.ru

The "zero power" ASTRA critical facility built in Kurchatov Institute [3-7] is intended for experimental investigations of neutron-physical peculiarities of modular HTGRs. It has been extensively used to simulate modular HTGRs of different designs, such as VGR-50 (developed in Russia), PBMR (being developed in RSA) and others. Experimental investigation at the ASTRA critical facility covers the following set of measurements:

1. Experimental investigation of spatial power density distributions (fission reaction rate measurements);
2. Measurements of the worth of safety rods mockups, their interference factor and calibration curves;
3. Measurements of neutron kinetic parameters (effective neutron lifetime);
4. Simulation of reactor physical startup.

Because of the "zero power" critical facility conditions, the uncertainties caused by material composition, temperatures and geometry uncertainties, are considerably lower than in power reactor. In absence of burning, slagging and poisoning effects, the uncertainty of the fuel isotopic composition depends only on the technology of fuel fabrication. This feature allows using the results of experiments to verify neutron-physical codes used in HTGR calculations [6, 7].

In HTGR design calculations it is supposed that the following approaches to flattening of power distribution could be used:

1. Placement of "heavy" poison rods in the inner reflector;
2. Placement of poison profiling elements at the boundary of active core and inner or side reflector;
3. Profiling of the outer layer of fuel elements by contents of burnable poison or fuel enrichment.

The primary goal of the present work is the performance of computational analysis of spatial distributions of fission reaction rates on the basis of available experimental data. The idea was to check one of the possible approaches to decrease the non-uniformity of power density distribution in the thin annular core, namely, by placement of additional poison rods in the inner reflector.

2. Experiments on Flattening of Power Density Distribution

In the experiments, the ASTRA facility configurations consisted of three radial zones: inner reflector made of graphite, annular core containing spherical fuel elements and side reflector made of graphite.

Investigation of the influence of poison rods, placed in the inner reflector, on the radial shape of ^{235}U fission reaction rates distribution was performed in three stages. At the first stage the core was loaded with a minimal number of spherical fuel elements to achieve critical state with minimum reactivity margin (configuration 1). In the critical state all reactivity compensation rods and safety rods were in their upper position out of the core. In this configuration the ^{235}U fission reaction rates distributions in radial direction (direction 8 in Fig. 1) and axial direction were measured. The measurements of control rods worth and their calibration curves (for the purpose of subsequent final load of assembly) were performed as well. At the second stage, a co-called "leave-in-place" poison rod (similar to the compensation and safety rods) was placed in the inner reflector; the height of the pebble bed core was increased and the second critical state was achieved (configuration 2). For this critical state the complete set of measurements was repeated. The third critical configuration was built on the basis of configuration 2 by placement of the second leave-in-place poison rod in the inner reflector. In configuration 3 the full set of measurements was performed once more.

Figure 1: Layout of Annular Core Assembly at the ASTRA Critical Facility

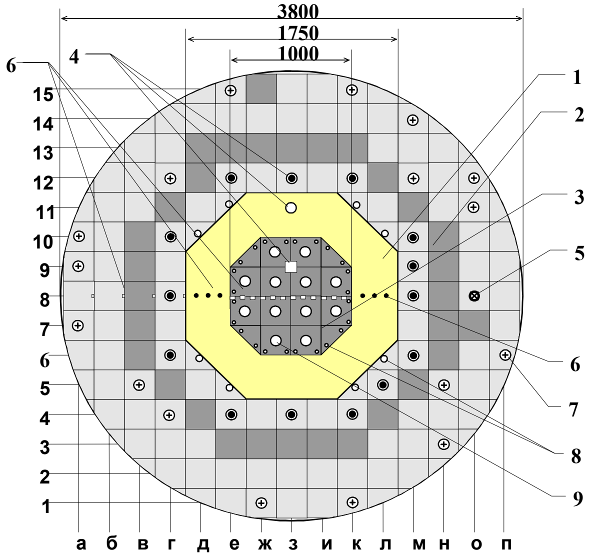

1- Annular core
2- Side Reflector
3- Inner Reflector
4- Control rod channels
5- Neutron source channel
6- Experimental channels for activation detectors
7- Channels for neutron counters and ionization chambers
8- Channels for poison profiling elements
9- Channels without plugs in IR blocks

Dimensions are given in mm

3. Computational Analysis

The computational analysis of the experimental data on spatial distributions of ^{235}U fission reaction rates was performed with the use of JAR [8, 9] and WIMS-D [10-12] design codes, currently applied in HTGR design calculations in Russia.

When performing fine-mesh full-core diffusion calculations with the JAR code, the neutron energy range was subdivided in 13 groups. To prepare macroscopic and microscopic 13 group neutron cross-sections, WIMS-D code was applied. Neutron thermalization was taken into account in the whole energy range below 4 eV.

During these calculational studies the technique of preparation of 13-groups macroscopic cross-sections for various components (physical zones) of the critical assembly was analyzed. The key attention was given to taking into account the neutron leakage from graphite blocks with axial cylindrical holes, pebble bed of fuel elements and pebble bed of graphite spherical elements in the top reflector.

Two series of calculation were performed. First series of 3D calculation was carried out with diffusion coefficients prepared traditionally, e.g. by averaging of transport cross-sections in the zones of an equivalent cell with weights of zone volumes and neutron flux (Standard option). Another series of calculations was carried out with axial diffusion coefficients, prepared by ARIADNE option of WIMS-D code. In the radial direction were applied diffusion coefficients prepared by the standard option.

The distinction between radial and axial diffusion factors was explicitly taken into account in JAR code during solution of the finite-difference neutron diffusion equation.

The results of calculations of neutron multiplication factors for all considered ASTRA configurations are presented in Table 1. In all these cases the assembly was in the critical state, and the uncertainty of experimental determination of the critical state did not exceed $4.2{*}10^{-6}$.

Table 1: Values of neutron multiplication factor for the considered configuration.

Configuration	1	2	3
JAR, WIMS (Standard)	1.01440	1.00917	1.01969
JAR, WIMS (Ariadne)	0.99662	0.99524	1.01089

Tables 2…5 present results of computational analysis of radial distributions of ^{235}U fission rates. When analyzing, the values of fission reaction rates were normalized by the average value. Fission rates distribution are presented in Figs 2-5.

Table 2: ^{235}U Fission Reaction Rates in Radial Direction (relative units) for Configurations 1…3.

R, cm (a)	Configuration 1			Configuration 2			Configuration 3		
	Expe-riment (relative units)	(C-E)/E, (S) (%) (b)	(C-E)/E, (A) (%) (c)	Expe-riment (relative units)	(C-E)/E, (S) (%) (b)	(C-E)/E, (A) (%) (c)	Expe-riment (relative units)	(C-E)/E, (S) (%) (b)	(C-E)/E, (A) (%) (c)
↓Side Reflector↓									
50	0.396	5.7	5.7	0.423	-6.0	-6.1	0.613	-9.8	-10.0
75	0.759	-1.8	-1.1	0.725	-4.4	-3.9	1.008	-5.6	-5.6
100	0.729	1.6	3.2	0.644	3.5	4.9	0.867	3.8	4.4
↓Core↓									
108.5	0.668	-8.2	-6.5	0.568	-5.3	-3.7	0.815	-11.6	-10.9
118.5	0.678	-8.0	-6.2	0.547	-4.9	-3.1	0.738	-7.1	-6.1
128.5	0.764	-8.1	-6.5	0.569	-4.7	-3.0	0.782	-10.2	-9.4
↓Inner Reflector↓									
139	0.918	9.4	10.4	0.630	10.5	11.8	0.768	14.1	14.8
147.3	1.257	-3.7	-3.5	0.700	12.9	13.3	0.849	13.2	13.4
155.6	1.252	6.1	5.8	0.878	7.8	7.7	1.142	-2.7	-2.8
164	1.369	2.9	2.2	1.126	3.9	3.3	1.270	4.4	4.1
172.3	1.443	-0.3	-1.4	1.356	-1.6	-2.5	1.473	-0.6	-1.2
180.5	1.432	1.5	0.2	1.447	0.3	-0.8	1.589	-3.5	-4.1
189	1.494	-2.3	-3.5	1.582	-1.6	-2.6	1.639	-4.9	-5.5
197.3	1.506	-3.8	-5.0	1.656	-2.0	-3.0	1.585	-3.8	-4.4
205.6	1.418	1.1	0.0	1.673	-0.7	-1.5	1.330	8.4	7.9
214	1.365	1.6	1.2	1.655	0.4	0.0	1.245	2.6	2.4
222.3	1.273	1.9	1.7	1.550	2.7	2.5	1.015	5.3	5.4
230.6	1.143	1.6	2.0	1.426	1.7	2.0	0.909	5.6	6.1
↓Core↓									
246.5	0.752	-6.0	-4.3	0.992	-8.2	-7.0	0.768	-7.0	-6.1
256.5	0.655	-4.8	-2.6	0.894	-8.7	-7.2	0.679	2.4	3.5
266.5	0.643	-4.8	-2.7	0.879	-7.9	-6.5	0.778	-6.5	-5.7

(a) Distance from the exterior surface of side reflector

(b) S -^{235}U Fission rates, calculated with using standard option

(c) A -^{235}U Fission rates, calculated with using ARIADNE option

Table 3: Integral Accuracy Parameters, Configuration 1

Region	Max(δE_i)		Average Percent Error		Root Mean Square of the Percent Error	
	Standard	Ariadne	Standard	Ariadne	Standard	Ariadne
Side Reflector	5.7	5.7	1.83	2.59	3.59	3.82
Core	-8.2	-6.5	-6.6	-4.8	6.81	5.08
Inner reflector	9.4	10.4	1.32	0.83	3.87	4.14

Table 4: Integral Accuracy Parameters, Configuration 2

Region	Max(δE_i)		Average Percent Error		Root Mean Square of the Percent Error	
	Standard	Ariadne	Standard	Ariadne	Standard	Ariadne
Side reflector	-6,0	-6,1	-2,3	-1,7	4,77	5,04
Core	-8,7	-7,2	-6,6	-5,1	6,81	5,41
Inner reflector	12,9	13,3	2,86	2,52	5,57	5,93

Table 5: Integral Accuracy Parameters, Configuration 3

Region	Max(δE_i)		Average Percent Error		Root Mean Square of the Percent Error	
	Standard	Ariadne	Standard	Ariadne	Standard	Ariadne
Side reflector	-9.8	-10.0	-3.85	-3.73	6.86	7.10
Core	-11.6	-10.9	-6.7	-5.8	8.02	7.38
Inner reflector	14.1	14.8	3.18	3.0	7.0	7.23

Figure 2: ^{235}U Fission Reaction Rate Radial Distribution for Configuration 1.

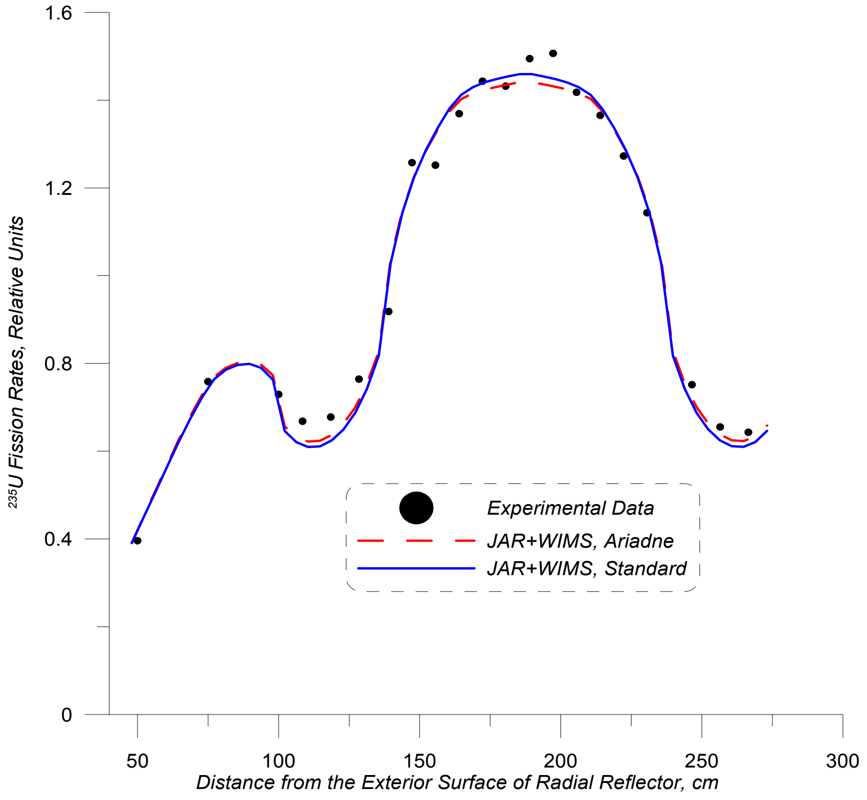

Figure 3: ^{235}U Fission Reaction Rate Radial Distribution for Configuration 2.

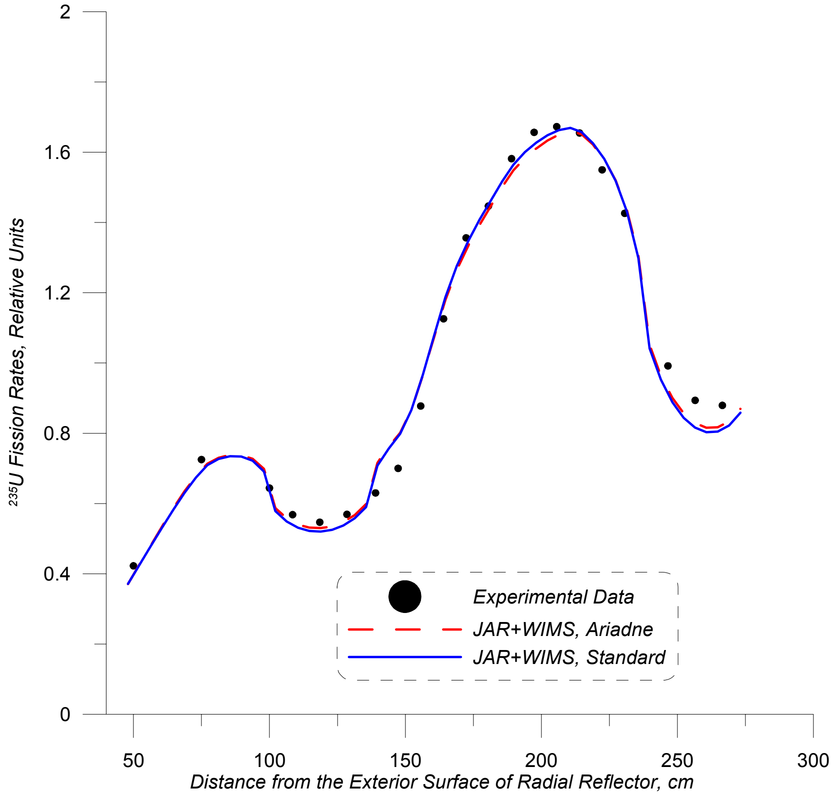

Figure 4: ^{235}U Fission Reaction Rate Radial Distribution for Configuration 3.

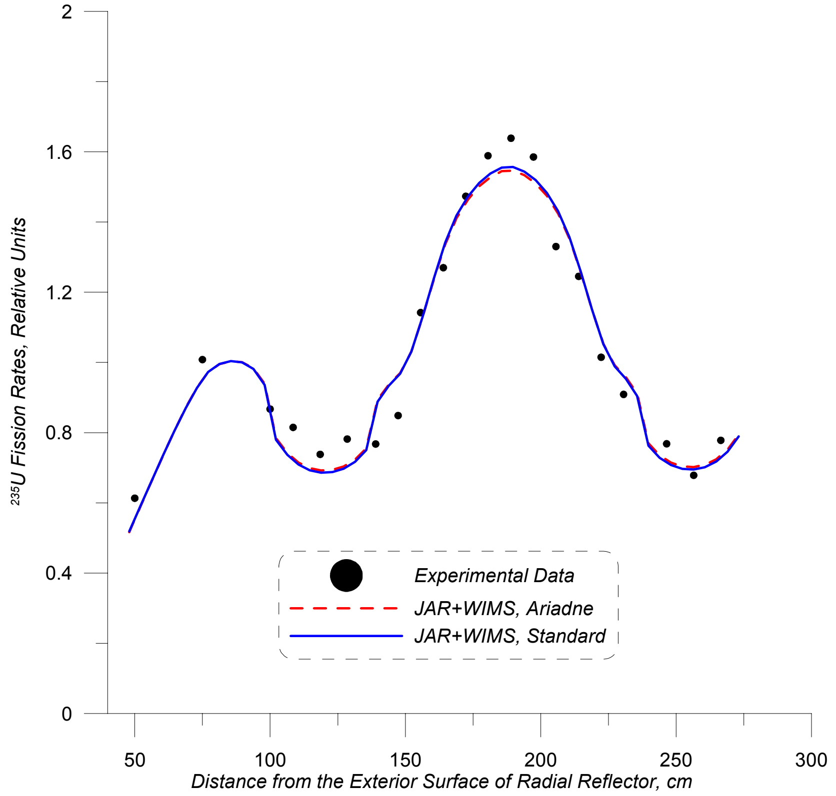

Figure 5: Calculated Radial Distribution of ^{235}U Fission Reaction Rate in the Active Core for Configurations 1…3, Depending on Number of Leave-in-Place Poison Rods (See Table 6), Inserted in the Inner Reflector.

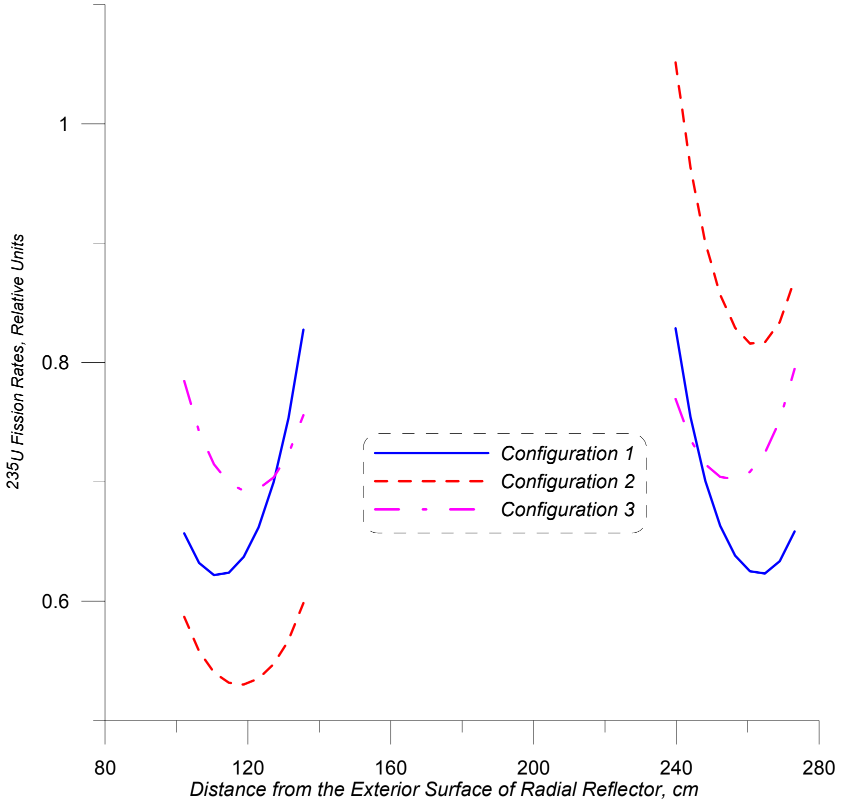

4. Discussion

Analysis shows that the application of both calculational techniques gives almost similar results. For the majority of positions in the inner reflector the deviation of calculated values from the experimental data does not exceed experimental errors of 5 % (with confidential probability range of 90 %). As a rule, the deviation value does not exceed 3 %. It should be noted that the regions in inner reflector close to the core and inner reflector boundary are the most difficult for calculations. In the mentioned regions the deviation of calculated fission reaction rate from the experimental data achieves 10-15 % (especially in the case of inserted leave-in-place poison rods in the inner reflector).

For the active core region, improved account for axial leakage (application of axial diffusion coefficients prepared using ARIADNE option) gives in average by 1 % smaller deviations from experimental data than in the case of standard option. However, in the case of two leave-in-place poison rods installed in the inner reflector (configuration 3), the value of deviation of calculated fission rates from the experimental data reaches 11 %. When only one leave-in-place poison rod is installed in the inner reflector (configuration 2) or without the installed leave-in-place poison rods (configuration 1), the deviation of ^{235}U fission reaction rates calculated with axial diffusion coefficients is about 5-6 %, thus exceeding the experimental error only by 1%. In the case when diffusion coefficients are prepared using the standard technique these deviations achieves 8 %.

In the side reflector, in the case of configuration 1 (absence of leave-in-place poison rods in the inner reflector) or configuration 2 (one leave-in-place poison rod is installed in the inner reflector) the maximum of deviation of calculated ^{235}U fission rates from experimental data does not exceed 6 %. When two permanent absorber rods installed in inner reflector, deviation achieves 10 %.

It should be noted, that analysis showed the increasing tendency of deviation of calculated values from experimental data with increase of numbers of leave-in-place poison rods placed into the inner reflector. This tendency is illustrated by Table 6. It is evident that influence of incorrectness in poison rod simulation on accuracy of fission rate calculations is stronger than influence of a method of leakage description in the graphite blocks with axial hollow channels.

Table 6: Root mean square of the of ^{235}U fission rates percent error distribution.

Configuration / Number of permanent absorber rods	1/0	2/1	3/2
JAR, WIMS (Standard) (%)	4.86	5.85	7.29
JAR, WIMS (Ariadne) (%)	4.39	5.67	7.25

It also should be noted that placement of “heavy” poison rods into inner reflector essentially decreases non-uniformity of the fission rate distribution compared with the configuration without poison rods in the inner reflector. Figure 5 shows that placement of one poison rod into the inner reflector decreases non-uniformity of fission reaction rate distribution in the region near the poison rod position and increases non-uniformity in the opposite region (configuration 2). Placement of two poison rods gives two practically symmetrical distributions. Difference between maximum and minimum values of the ^{235}U fission rate is significantly smaller than in configuration 1 without poison rods in the inner reflector.

Thus, the calculated distributions of ^{235}U fission rates are close to the experimental data, obtained at the ASTRA critical facility. This fact ensures the principle possibility to use JAR and WIMS-D codes in HTGR design calculations for solving the problem of power distribution flattening by means of searching optimal positions for poison rods placement.

5. Conclusions

In present work we implemented computational analysis of results of experimental studies on power density distribution in a HTGR reactor with the annular core. An approach to flatten the radial power distribution by means of placement of poison rods in inner reflector was investigated.

Typical and maximum deviations of calculated fission reaction rates from experimental data were determined. It was shown, that there is a tendency of increasing the deviation of calculated values from experimental data with increase of the number of “leave-in-place” poison rods placed into the inner reflector.

References

1) A.I. Kiriushin, N.N. Ponomarev-Stepnoi, E.S. Glushkov et al., “Project of the GT-MHR high-temperature helium reactor with gas turbine”, Nucl. Eng. and Design 173, p. 119-129 (1997).
2) E.J. Mulder, “Pebble Bed Reactor with Equalized Core Power Distribution Inherently Safe and Simple”, Forschungszentrum Jülich, JÜL-3632, (Jan. 1999).

3) A.A. Bykov, A.Yu. Gagarinski, E.S. Glushkov et al., “Programs of experiments with critical assemblies at the Russian Research Centre “Kurchatov Institute””, Nucl. Sci. and Eng., v. 145, p. 181–187, (2003)
4) N.N. Ponomarev-Stepnoi, N.E. Kukharkin, E.S. Glushkov et al., “Experiments on HTR criticality parameters at the ASTRA facility of the Kurchatov Institute”, Nucl. Eng. and Des., v. 222, p 215–229, (June 2003)
5) N.N. Ponomarev-Stepnoi, N.E. Kukharkin, E.S. Glushkov et al., “Experiments on ASTRA critical facility on justification of neutron-physical parameters modular HTGR”, RRC “Kurchatov Institute”, preprint IAE–6340/4, Moscow, Russia, (2004) (in Russian).
6) N.N. Ponomarev-Stepnoi, V.I. Bryzgalov, E.S Glushkov et al., “Application of MCU code to computational analysis of critical experiments with HTGR spherical fuel elements at ASTRA facility”, Atomnaya Energia, v. 97 (4), p.243─252, (2004) (in Russian).
7) V.D. Davidenko, V.F. Tsibulsky, “Calculations of efficiency control rods of ASTRA critical facility”, Proc. of “Codes and algorithms for neutron-physical calculations of nuclear reactors” (Neutronics-96), Obninsk, Russia, p.65-68, (1998) (in Russian).
8) L.N. Yaroslavtseva, “Program complex JARB for calculations of neutron–physical parameters of nuclear reactors”, VANT, series “Physics and nuclear reactor engineering”, v. 8 (37), p. 41-43, (1983) (in Russian)
9) L.N. Yaroslavtseva, P.A. Fomichenko, P.N. Alekseev, “Verification on stationary and time-depended algorithms in program complex JAR”, Proc. of “Codes and algorithms for neutron-physical calculations of nuclear reactors” (Neutronics-92), Obninsk, Russia, p.34-37 (1994) (in Russian).
10) J.R. Askew et al., “A General Description of the Lattice Code WIMS”, JBWES, (Oct. 1966).
11) WIMSD5, NEA Data Bank Documentation, No. 1507/02, (1996).
12) WLUP - WIMS Library Update. IAEA Final Report of a Coordinated Research Project, (2003).